ELT-HIRES the high resolution spectrograph for the ELT: implementing exoplanet atmosphere reflection detection with a SCAO module

Marco Xompero, Christophe Giordano, Marco Bonaglia, Gianluca Di Rico, Guido Agapito, et al.

Marco Xompero, Christophe Giordano, Marco Bonaglia, Gianluca Di Rico, Guido Agapito, Simone Esposito, Andrea Tozzi, Nicoletta Sanna, Ernesto Oliva, Alessandro Marconi, "ELT-HIRES the high resolution spectrograph for the ELT: implementing exoplanet atmosphere reflection detection with a SCAO module," Proc. SPIE 10703, Adaptive Optics Systems VI, 1070341 (18 July 2018); doi: 10.1117/12.2309951

SPIE.

Event: SPIE Astronomical Telescopes + Instrumentation, 2018, Austin, Texas, United States

ELT-HIRES the high resolution spectrograph for the ELT: implementing exoplanet atmosphere reflection detection with a SCAO module

Marco Xompero[(a)],Christophe Giordano[(a)], Marco Bonaglia[(a)], Gianluca Di Rico[(b)], Guido Agapito[(a)], Simone Esposito[(a)], Andrea Tozzi[(a)], Nicoletta Sanna[(a)], Ernesto Oliva[(a)], Alessandro Marconi[(a)(c)]

[(a)]INAF - Osservatorio Astrofisico di Arcetri, Largo E. Fermi 5, Firenze, Italy
[(b)]INAF – Osservatorio Astronomico d'Abruzzo, Via M. Maggini, Teramo, Italy
[(c)] Dipartimento di Fisica e Astronomia, Università di Firenze, via G. Sansone 1, 50019 Sesto F.no (Firenze), Italy

ABSTRACT

The HIRES-ELT instrument foresees an observing mode that delivers integral field high resolution spectroscopy with spatial sampling down to the diffraction limit of the ELT telescope. The IFU-SCAO module presented here is sub-system of the front-end of HIRES-ELT that includes two modules: SCAO and IFU. The first is the wavefront sensor, based on a pyramid beam-splitter, that provides the guiding on the reference star and the analysis of the incoming wavefront; the second is the module that transforms the incoming f/17.7 light beam from the telescope to the appropriate f/numbers to feed the spectrometer fibers-array with the required spatial scale. In this paper, we will present the SCAO optical design to allow the exoplanet atmosphere detection in reflection. To achieve this goal, we studied a feasible pyramid wavefront sensor to be inserted in a sliding arm of the HIRES front end. The CCD camera is based on a CCD220 chip in which will be imaged the telescope pupil, sampled with a 90x90 sub-aperture grid. A total of 4089 Karhunen-Loëve modes have been generated and used to close an end-to-end simulation. The AO loop runs up to 1000 KHz and it allows to shrink the PSF to the diffraction limits of the telescope ant to achieve Strehl Ratio (SR) above 70% in best seeing case up to magnitude 15 in H-band and a SR permanently above 40%, same band, up to magnitude 14 in case of median seeing. For λ=1600nm the 50% of energy is reached before 1 λ/D for all the plotted I-magnitude under the best seeing conditions. Under Median seeing conditions, the 50% is reached before 2λ/D up to I-mag 13. For λ=1000nm instead, we reach the 50% of encircled energy before a radius of 2λ/D for I-mag less than 14 and after 5λ/D for I-mag greater than 15 in the best seeing case. For each IFU spatial sampling and resolution, we can reach a contrast of 10^3 at a distance of 4 spaxels from central peak.

Keywords: ELT, HIRES, SCAO, IFU, PSF, contrast, exoplanet detection

1. INTRODUCTION

The IFU-SCAO module collects the light coming from the ELT [1] and injects it into the bundles of optical fibers corresponding to the selected observing mode. The module is composed by two different subsystems optically separated by a dichroic window:

- **SCAO module.** It is the wavefront sensor, based on a pyramid sensor [2][3][4], that will provide the guiding on the reference star and the analysis of the incoming wavefront.
- **IFU module.** It is the module that will transform the incoming f/17-7 light beam to the appropriate f/# to feed the micro-lenses placed on the input side of the fibers, arranged in a rectangular configuration. [5].

2. GENERAL PHYSICAL DESCRIPTION

1.1 Physical architecture

The IFU-SCAO is located into the Nasmyth de-rotator structure as visible in Figure 1: it is a gravity variant box of 1250x1150x750 mm where the two subsystems are placed one over the other.

Adaptive Optics Systems VI, edited by Laird M. Close, Laura Schreiber, Dirk Schmidt, Proc. of SPIE Vol. 10703, 1070341 · © 2018 SPIE
CCC code: 0277-786X/18/$18 · doi: 10.1117/12.2309951

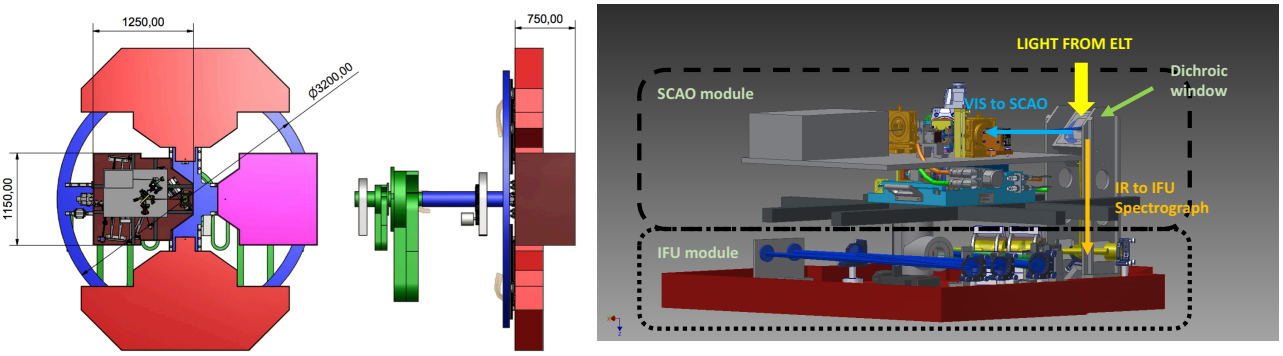

Figure 1 (left) The IFU-SCAO module is located into the Nasmyth rotator structure. (right) Mechanical 3D view of the module

The box is placed on a translation stage, visible on the left side of the brown box, to have the possibility to be used alternatively with the other modules (in red and pink in figure)[13]. Following on the right, the mechanical design of the IFU-SCAO module is visible. It is composed by the two subsystems: looking at the figure in the bottom part of the box there is the IFU module fed by the transmitted IR light (950-2400 nm) by the dichroic window, while the SCAO module is placed on the top part of the same box and fed by the reflected bluer light (400-950nm).

The SCAO module coupled with IFU unit will open a new scientific branch in the science cases of HIRES. In fact, the module us to detect and characterize the atmosphere of the exoplanet by means through reflected light spectroscopy [6]. The angular resolution of the ELT in AO-assisted mode will enable a breakthrough in this approach, since exoplanets in close-in orbits around nearby stars will be resolved for the first time. This new technique [7] does not require that the exoplanet is directly detectable in imaging: first, the AO system enhances the planet-to-star contrast at the planet location, and then high-resolution spectroscopy disentangles the planetary and stellar spectra. This is within the reach of HIRES provided the AO system can deliver a contrast enhancement of ~1000 at a few λ/D.

3. SCAO MODULE

The SCAO module for HIRES is based on a pyramid WFS. The design followed the concepts started with the LBT FLAO [8] systems and followed by the Magellan MagAO system [9]. Such WFS, coupled with a voice coil deformable mirror as M4 for ELT [10], proved to achieve very high performances and contrast even in infrared and visible band. The module (Figure 2) is mounted on an aluminum board 800x600 mm placed on a double axis stage that allows the whole relay optics to move along X and Z axis to adjust the focus and to provide off axis capabilities to the adaptive optics corrections. The light coming from the dichroic is directed to the top of a square based glass pyramid and the four resulting pupils are focused on the ALICE ESO camera.

The active components in this design are:

- *Positioning stages*: they are located below the WFS board and are used to follow the telescope focus and to allow the patrolling of the whole SCAO module in one direction. The stages are bolted in one side to an aluminum support frame that is holding the SCAO module. It will allow displacement of 45mm in both directions (about 3 arcsec on sky) along X axis and 20 mm of travel range along Z axis for focusing capabilities.
- *Technical camera*: it is a Gigabit Ethernet wide field camera (about 10 arcsec on sky) to help the pointing operation during the close loop setup. With this feedback, the SCAO module can ask to the telescope and to the positioning stage the alignment corrections to have the beam focused on the top of the pyramid. It is a 4.2 Megapixel CCD camera (2048x2040 pixels, 7.4um size per pixel, 12-bit ADC resolution) operating up to 15 frames per second.
- *Tip tilt mirror*: the mirror main function is to modulate the spot on the top of the pyramid in order to uniformly illuminate the four faces and allow the sensing of the wavefront. It has high resonant frequency and about two mechanical degrees of stroke in both tip and tilt axis. This high tip tilt mirror range allows an off-axis capability for the system of few arcsec (<2 arcsec diameter)

- *ADC*: is composed by two rotating stages that will correct for the atmospheric dispersion. A couple of optics, aligned by the stages, are rotated following the elevation angle in order to compensate for the light dispersion introduced by the different thickness of the atmospheric layer seen by the telescope. Each module allows a continuous full rotation with a resolution of 0.75 arcmin.
- *K-mirror*: a single stage is used to rotate the K-mirror and to allow a pupil de-rotation. This is intended to keep fixed the map between the WFS sub-apertures and the corrector actuator while the telescope is tracking a reference star. The resolution and the minimum increment is about 350 micro-rad with a repeatability ten times better.
- *Camera lens*: it is used to focus the four pupils on the ESO ALICE CCD. The motorized movements are used to keep fixed the pupils position against the wobbling induced by the K-mirror, the rotating FE and the others misalignment sources. The selected product has as maximum travel range on both axis of 400 um and a resolution of <1 nm.
- *ALICE CCD camera*: ALICE is a codename for CCD220 based ESO development camera, used as placeholder for simulations and design.

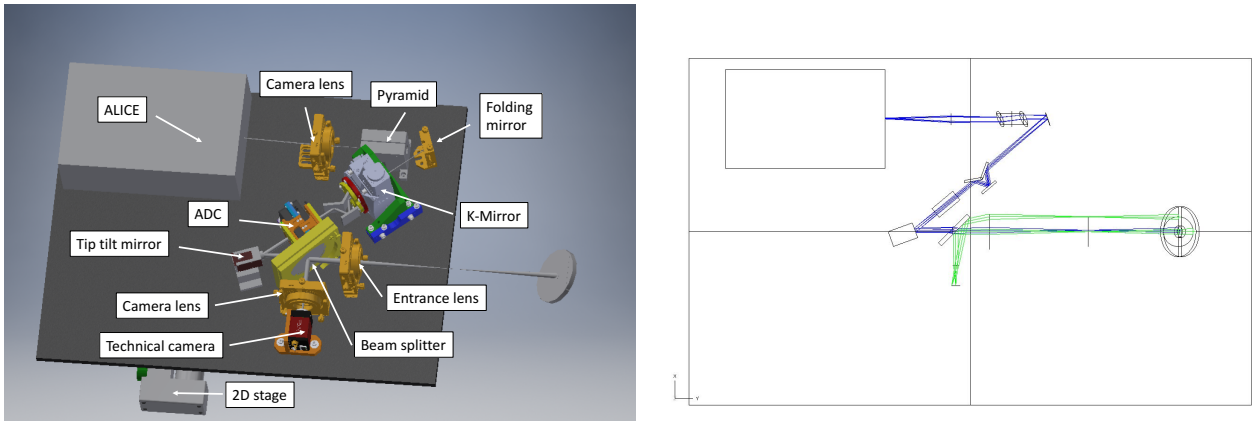

Figure 2: (left) SCAO module components overview and (right) Optical layout of the SCAO WFS. Green color highlights the TV channel light path while blue color the WFS channel.

The Figure 2 shows the optical layout of the SCAO WFS unit. The sensor FoV will be limited by the physical dimension of the glass double-pyramid that is constrained by manufacturing capabilities. Following the light path the main elements of the SCAO WFS are:

- The input lens (L1) that produces a F53.1 beam out of the F17.7 coming from the telescope. This solution will ease the manufacturing of the glass double-pyramid. Indeed, to not introduce non-linear effects in the WF measurements, the prism edges manufacturing imperfections must be smaller than ~1/10 of the PSF size (equivalent to 1 um on the F17.7 focal plane and 3 um on the F53.1). The L1 will also re-image the ELT pupil on the tip-tilt mirror, with a diameter of 10 mm.
- The Technical Viewer (TV) dichroic. This will be a dichroic, or movable fold mirror, used to feed light into the TV camera during the NGS acquisition procedure.
- The TV camera lens produces a faster beam out of the F53.1 used on the WFS channel. It is required to shrink the 10” focal plane on the TV camera chip (of ~15 mm side).
- The tip-tilt mirror: this is just a 10 mm diameter, 2 mm thick flat mirror that folds light at 20° AOI. The mirror will be mounted on a piezo-actuated tip-tilt platform to produce the PSF modulation on the pyramid focal plane required to adapt the WFS dynamic range and sensitivity. This element will be placed in a plane optically conjugated to the system pupil in such a way that when the modulation is applied to the platform, the 4 pupil images generated on the detector by the WFS camera lens will not wobble, preserving the correlation between WFS sub-apertures and DM actuators.
- ADC: at the current design state this element is just a place-holder, made out of a 60 mm thick BK7 glass rod

- The K mirror: this element is made out of 3 flat mirrors with 60° - 30° -60° AOI respectively. It is mounted on a rotating stage to allow for the pupil de-rotation. This is the typical design for pupil de-rotation adopted in FLAO, ERIS and GMT NGWS.
- The WFS fold mirror: it is a simple flat mirror of 1" diameter used to compact the WFS layout.
- The double pyramid: it represents the core of the WFS and is the sensing optics.
- The camera lens is an achromatic doublet lens used to re-image the system pupil on the WFS detector. It will be placed on an actuated XY stage to adjust the 4 pupils on the detector array compensating for the opto-mechanical misalignments of the system.

4. AO SYSTEM SIMULATION

To estimate the HIRES AO system performances, we performed numerical simulations using the library PASSATA [11] developed by the INAF-Arcetri AO team.

The AO parameters considered in our simulations are:

- Telescope size (Diameter: 39.146m, Central obstruction: 0.287, Pupil as shown in the Figure 3)
- Wavelength: chosen λ=798nm (I-band) with a bandwidth of 155nm (then 720nm < λ < 875nm) to be out of the other band considered. The performance analysis has been done for λ=1000 nm and λ=1600 nm.
- Atmospheric conditions: Seeing at z=30º of 0.471" for the best seeing case and 0.793" for the median seeing case. The Sky background in I-band (λ=798nm) was set to 101.49 detected photons/m^2/$arcsec^2$/s (given without considering the atmospheric and instrumental transmission)
- Light transmission: Atmospheric + telescope transmission: 0.6261, Warm optics + WFS optics: 0.68, Quantum efficiency of the camera: 0.85
- Deformable mirror: Simulated, with 4096 influence function (IFs)
- Guide star: NGS: magnitude explored between I=8 and I=15
- WFS camera detector: OCAM2K, with RON value: 0.3 e^-/pix/frame, Dark current: $0.444/f_s + 0.00556$ e-/pix/frame (fs = detector frequency) and Charge diffusion: Gaussian with a FWHM = 0.55 pixel corresponding to a loss of 6%
- NGS WFS: 90x90 sub-apertures Pyramid, with Sub-aperture FoV: 2.1x2.1 arcsec
- AO RTC: 1000Hz Maximum frequency; Modal control with static modal gains and modal base made of Zernike Tip, Tilt, Focus and astigmatism and higher order 4089 Karhunen-Loëve (KL) modes fitted on the influence functions.
- The number of controlled modes is optimized in the simulation.
- Temporal controller: Simple integrator (gain optimized in the simulation)
- Vibrations error: 2 RMS jitter
- The High Spatial Frequency (HSF) error defined in the ESO package is included as a phase screen at the pupil height (Figure 3)

It has been decided to not consider the M4 segmentation and the spider arms in this phase.

The performance optimization was done by exploring the free parameters for each NGS magnitude considered and by searching the configuration giving the best Strehl Ratio.

We explored all possible permutations of the set of parameters summarized in Table 1

Table 1 Parameters to optimized and values explored.

Parameter	Values explored
CCD frame rates F [Hz]	1000, 800, 600, 500, 300, 200

Number of corrected modes	4094, 3827, 3654, 3402, 3159, 2925, 2700
Pyramid modulation amplitude [λ/D]	From 2 to 10 with a step of 0.5λ/D

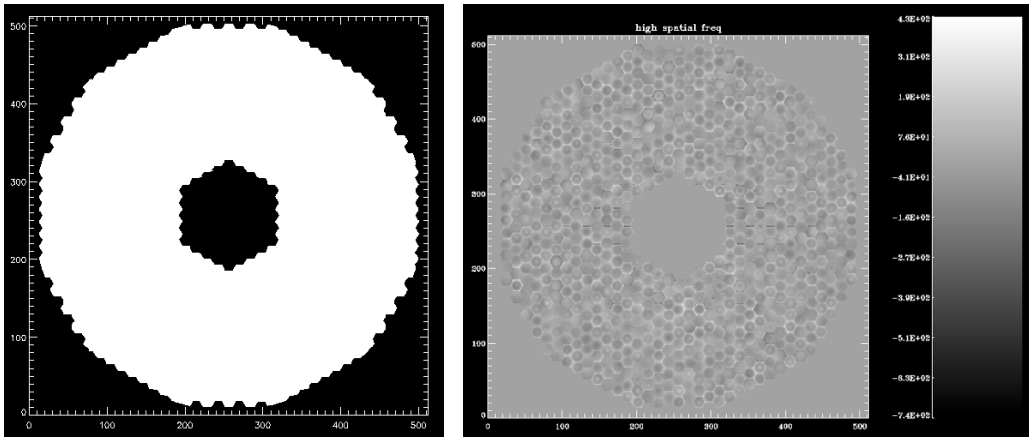

Figure 3 Pupil of the E-ELT (left) and High spatial frequency error sample(right).

For computational limitations, we have decided to proceed by following these assumptions as starting point of the optimization:

- The brightest magnitude should have a mode number close or equal to the maximum available
- The magnitude X+1 (fainter) should work with at most the same number of modes and the same frequency than the magnitude X.
- We start by choosing a smaller set of modulation amplitude: if a maximum Strehl ratio is reached inside this smaller set, excluding the boundary values, we consider the optimization of the modulation amplitude done. Otherwise, we enlarged the set of values in the direction where the Strehl ratio was found higher.

We optimized the modal gain at 1Hz and the optimization of the integrator was based on the work of [12]

We ran for every case a single realization simulation of 8s and we discard the first 4s to avoid transient effects and consider only the steady state. Figure 4 shows the summary of the best performances achieved with the parameters shown in Table 2.

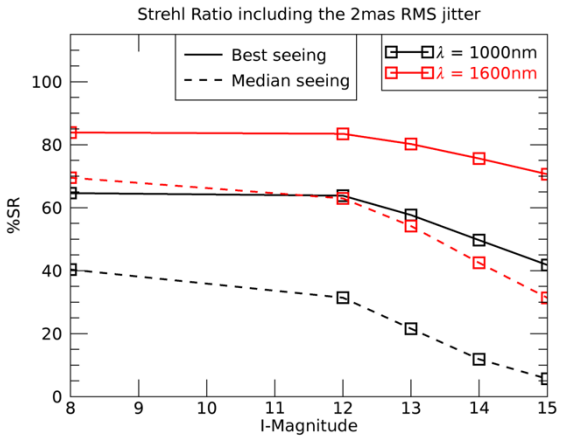

Figure 4 Strehl Ratio for best seeing case (solid lines) and median seeing case (dashed lines).

Table 2. Summary of the optimized parameters and of the fluxes of the NGS Pyramid WFS.

Cases		Best seeing					Median seeing				
I-mag		8	12	13	14	15	8	12	13	14	15
fr. [Hz]		1000	800	800	800	800	1000	1000	800	800	600
no. modes		4094	4094	3827	3654	3402	4094	4094	3827	3654	3402
Modulation amplitude [λ/D]		7.0	5.5	6.0	7.0	7.0	5.0	3.0	2.5	3.0	4.0
Flux [ph/sa/frame]		402.3	12.63	5.03	2.00	1.06	402.3	10.10	5.03	2.00	1.06
σ_R [e-/sa/frame]		0.6	0.6	0.6	0.6	0.6	0.6	0.6	0.6	0.6	0.6
σ_D [e-/sa/frame]		0.024	0.024	0.024	0.024	0.025	0.024	0.024	0.024	0.024	0.025
σ_B [e-/sa/frame]		0.024	0.03	0.03	0.03	0.04	0.024	0.024	0.03	0.03	0.04
SNR		14.18	2.49	1.55	0.95	0.66	14.18	2.22	1.55	0.95	0.66
Strehl ratio (W/o 2mas jitter)	λ = 1000nm	64.6 (73.0)	63.8 (72.1)	57.6 (65.1)	49.7 (56.1)	41.8 (47.0)	40.3 (45.5)	31.4 (35.3)	21.6 (24.2)	11.9 (13.2)	5.6 (6.2)
	λ = 1600nm	83.9 (88.2)	83.5 (87.8)	80.2 (84.4)	75.6 (79.6)	70.6 (74.2)	69.5 (73.0)	62.9 (66.1)	54.2 (56.8)	42.5 (44.5)	31.4 (32.7)

The SCAO system can guarantee a Strehl Ratio (SR) above 70% in best seeing case up to magnitude 15 in H-band and a SR permanently above 40%, same band, up to magnitude 14 in case of median seeing. Noticeable is the SR foreseen going to the visible in Y band, in which the SR is still very high in best seeing conditions at almost all the considered magnitude and up to magnitude 13 in median seeing conditions. The telescope residual jitter has been considered by convolving the resulting PSF with a 2 mas Gaussian. The values between parentheses, reported for comparison, are taken before the convolution.

Quality of the correction

To understand the quality of adaptive optics loop correction we decomposed the input phase screen and the residual wavefront with the KL modal base and we analyzed the plot for each magnitude and each seeing case (see Figure 5). These curves are the standard deviation of both the turbulence modal (black) and the modal residues (red).

These figures show that all the 4094 modes are well corrected for I-mag =8 and I-mag = 12, as we expect. For I-mag= 15 the residual curve converges to the turbulence curve, showing that modes above 3402 are not corrected (see Table 2). A sign of the goodness of the loop correction is the fact that the residual is always below the turbulence: that indicates there are no oscillation or uncontrolled modes that could bring the loop to instability.

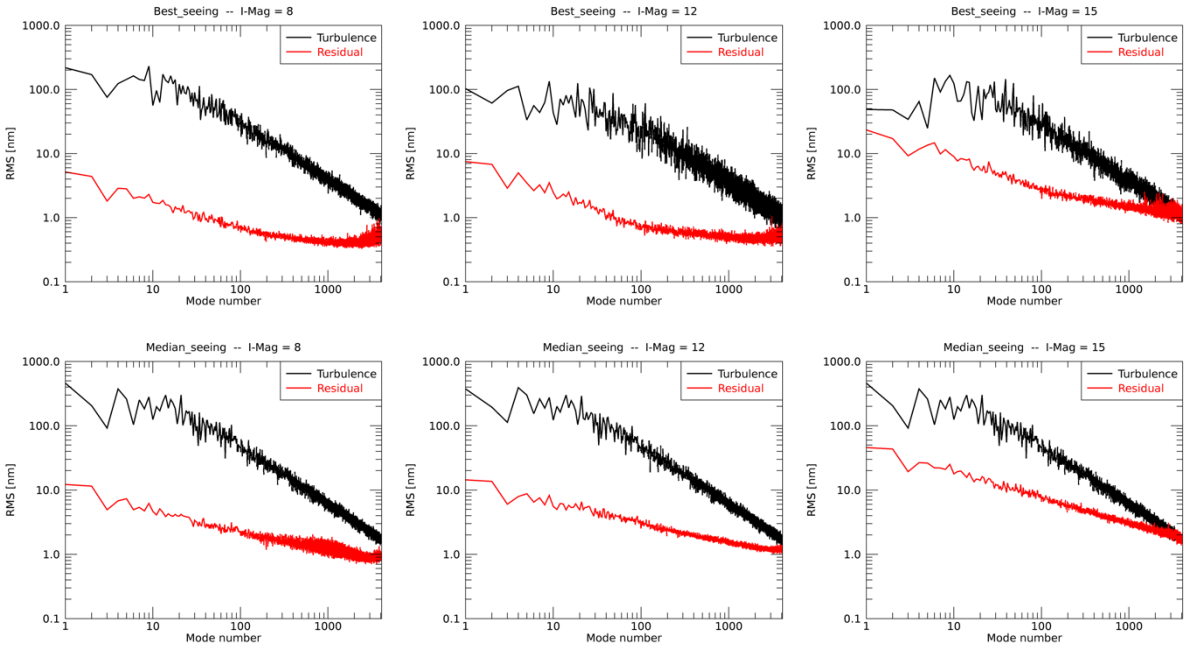

Figure 5. Modal plot in the best seeing (top) and median (bottom) conditions for, from the left to the right, magnitude 8, 12 and 15.

5. RESULTS

From the simulation data, we computed the long exposure PSF and their mean profile for each case, changing magnitude, wavelength and atmospherical seeing. The Figure 6 shows these profiles and the comparison with the seeing limited case: the PSF profiles, in fact, at a certain distance from central core, drop to the seeing limited case because uncorrected.

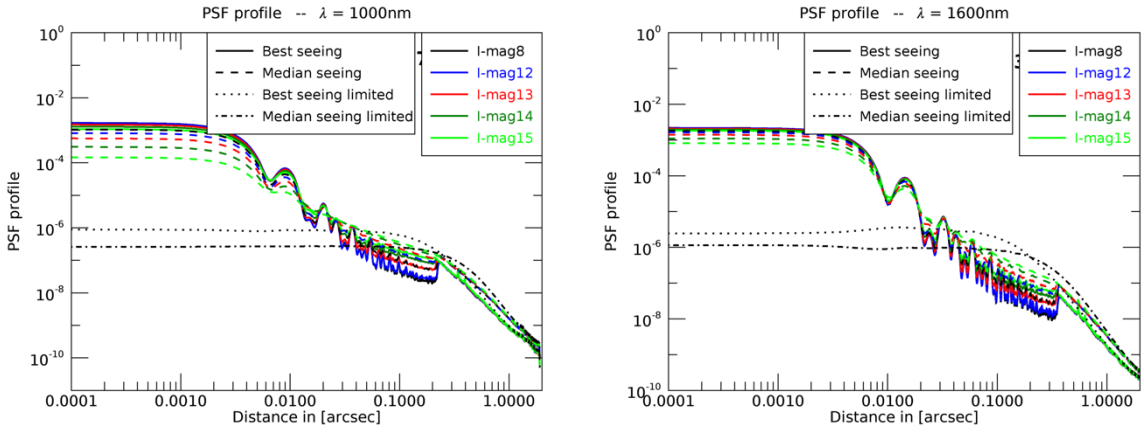

Figure 6 Mean profiles of the non-normalized PSFs under different conditions and for different wavelengths (left: λ = 900nm and right: λ = 1600nm)

Then we normalized the PSFs to its central peak and we compute their mean profiles (see Figure 7) and encircled energy (see Figure 8). It is clear that, for λ=1000nm, we reach the 50% of encircled energy before a radius of 2λ/D for I-mag less than I-mag ≈ 14 and after 5λ/D for I-mag ≥ 15 in the best seeing case. The median seeing case doesn't allow to reach the 50% of energy in the plotted range.

For λ=1600nm the 50% of energy is reached before 1λ/D for all the plotted I-magnitude under the best seeing conditions. Under Median seeing conditions, the 50% is reached before 2λ/D up to I-mag ≈ 13.

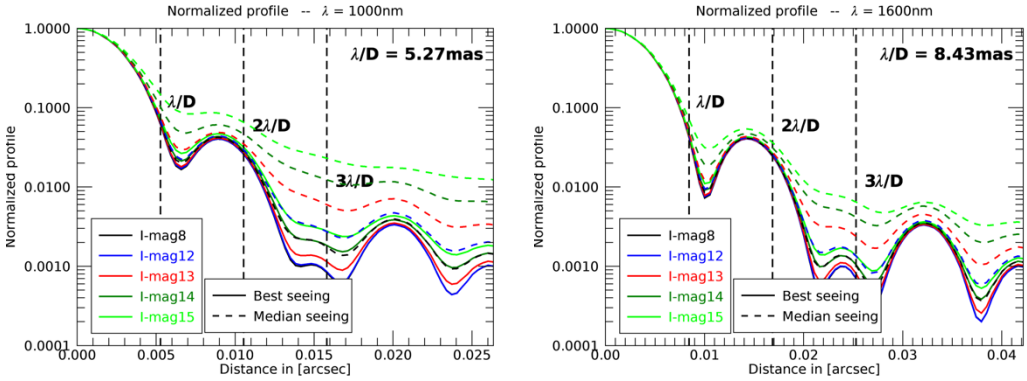

Figure 7 PSF profiles normalized by the central peak of the long exposure PSF for different wavelengths: 1000nm (left) and 1600nm (right) and the two seeing cases: best (solid lines) and median (dashed line).

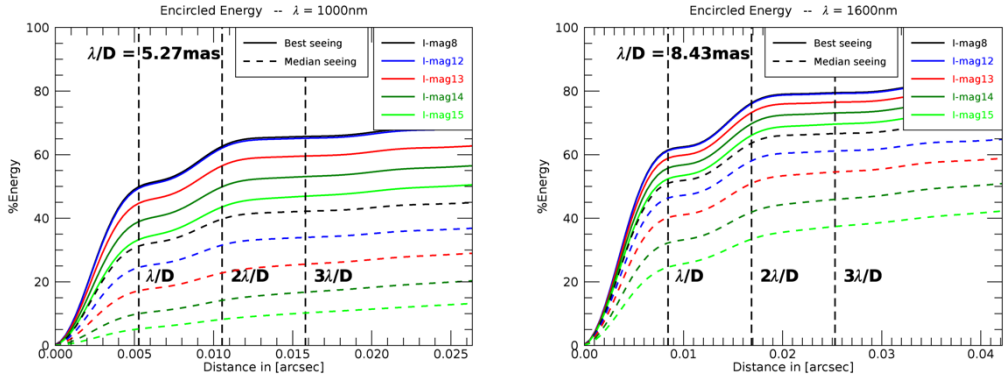

Figure 8 Encircled energy for the three different wavelengths: 1000nm (left) and 1600nm (right) and the two seeing cases: best (solid lines) and median (dashed line).

Since the IFU is supposed to work with different pixel scales (6.7, 10.0, 67.0, and 100.0 mas) we sampled the PSF as seen by the four IFU modes (obtained by two different f/# configurations and named IFU010 and IFU100) in order to evaluate the contrast achievable at different distances. As first we sampled the PSF at IFU scales changing the pixel scale and therefore we normalized the PSFs to the central peak . To evaluate the results, we chose a cut on two directions, corresponding approximately to the worst case (0˚) ant the best case (45˚) in the direction selection of the PSF 2D profile. The lowest magnitude and wavelength profile is on Figure 9.

The profiles are very interesting from many point of views.

First of all, we can state that for the best and median seeing, the correction is stable and good until about 0.6 arcsec, in which the pupil features start to be relevant respect to the PSF value. In particular, the worst cut shows above 0.6 arcsec, noisy signals, not dependent on the magnitude, that are clearly visible in case of high resolution IFU sampling. In the low resolution IFU sampling they are averaged out.

By design the complete IFU FoV is limited to 0.8 arcsec for IFU100 and to 0.07 arcsec to IFU010 so we will not have the issue of fall in the worst part of the PSF profile[5].

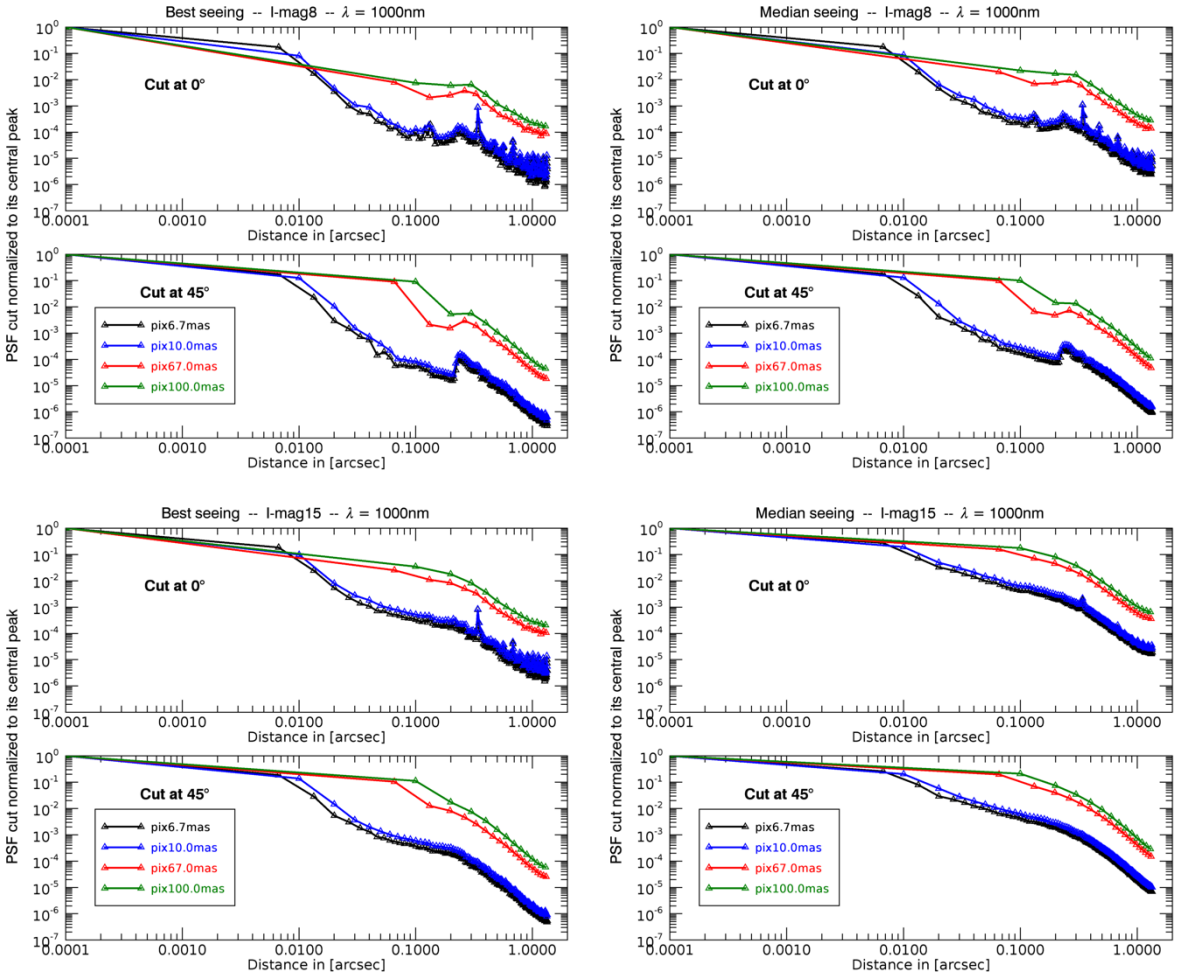

Figure 9 PSFs cut in two different direction (0°=worst, 45°=best) for the best seeing (left) and the median seeing (right) cases at λ=1000nm, mag 8 and 15.

In the best seeing case, with both PSF profile cut, we can reach after 4 spaxels a contrast of the order of 10^{-3} with the design as it is, as requested by the scientific case that is driving the instrument construction. The figures report only lower wavelength which is the worst case in terms of SCAO correction. For the other magnitudes and wavelength, we are in any case between 10^{-2} and 10^{-3} that is absolutely good starting point for the next phases of the project.

REFERENCES

[1] Tamai, Roberto et al.; "The E-ELT program status", Proceedings of the SPIE, Volume 9906, id. 99060W 13 pp. (2016)

[2] Ragazzoni R., Farinato J., "Sensitivity of a pyramidic Wave Front sensor in closed loop Adaptive Optics", Astronomy and Astrophysics, v.350, p. L23-L26 (1999)

[3] Esposito, S. et al., "Large Binocular Telescope Adaptive Optics System: new achievements and perspectives in adaptive optics" Proceedings of the SPIE, Volume 8149, id. 814902 (2011)

[4] Close, L.et al., "Into the Blue: AO Science in the Visible with MagAO", Proceedings of the Third AO4ELT Conference. Firenze, Italy, May 26-31, 2013

[5] Tozzi, A. et al. "ELT-HIRES the High Resolution Spectrograph for the ELT: the IFU-SCAO module", SPIE 2018, in press.

[6] Marconi, A. et al.; “EELT-HIRES the high-resolution spectrograph for the E-ELT”, Proceedings of the SPIE, Volume 9908, id. 990823 12 pp. (2016)
[7] Snellen, I. et al.; “Combining high-dispersion spectroscopy with high contrast imaging: Probing rocky planets around our nearest neighbors”, Astronomy & Astrophysics, Volume 576, id.A59, 9 pp.
[8] Quirós-Pacheco, F. et al.; “First light AO (FLAO) system for LBT: performance analysis and optimization”, Proceedings of the SPIE, Volume 7736, id. 77363H (2010)
[9] Morzinski, Katie M. et al.; “MagAO: Status and on-sky performance of the Magellan adaptive optics system”, Proceedings of the SPIE, Volume 9148, id. 914804 13 pp. (2014)
[10] Vernet, E. et al.; “On the way to build the M4 Unit for the E-ELT”, Proceedings of the SPIE, Volume 9148, id. 914824 10 pp. (2014)
[11] Agapito, G. et al.; “PASSATA: object oriented numerical simulation software for adaptive optics”, Proceedings of the SPIE, Volume 9909, id. 99097E 9 pp. (2016)
[12] Gendron, E.; Lena, P.; “Astronomical adaptive optics. 1: Modal control optimization”, Astronomy and Astrophysics (ISSN 0004-6361), vol. 291, no. 1, p. 337-347
[13] Cabral, A.; Aliverti, M; Coehlo, J.; et al.; “ELT-HIRES the high resolution spectrograph for the ELT: the design of the front end”, SPIE, 10702-358 (2018); in press